



# Fluorescence turn-on probe for biothiols: intramolecular hydrogen bonding effect on the Michael reaction

Hyun-Joon Ha<sup>a</sup>, Doo-Ha Yoon<sup>b</sup>, Seokan Park<sup>b</sup>, Hae-Jo Kim<sup>b,\*</sup>

<sup>a</sup> Department of Chemistry and Protein Research Centre for Bio-Industry, Hankuk University of Foreign Studies, Yongin 449-719, Republic of Korea

<sup>b</sup> Department of Chemistry, Hankuk University of Foreign Studies, Yongin 449-719, Republic of Korea

## ARTICLE INFO

### Article history:

Received 24 June 2011

Received in revised form 30 July 2011

Accepted 1 August 2011

Available online 6 August 2011

### Keywords:

Biothiol

Coumarinyl enone

Fluorescence

Hydrogen bond

Michael addition

## ABSTRACT

Weakly fluorescent coumarinyl enones are rapidly transformed into strongly fluorescent molecules through the Michael addition reaction of a thiol group, where an intramolecular hydrogen bond plays a critical role in the reaction rate. The molecular probe (**3**) with an *ortho* hydroxyl group to a carbonyl group exhibits a rapid response toward GSH owing to the stabilization of the possible oxyanion intermediate by a preferable intramolecular hydrogen bond. Probe **1** with an *o*-hydroxyl group also showed a moderately enhanced reaction rate with GSH and soluble in HEPES buffer to exhibit a highly selective and sensitive fluorescence turn-on response toward biothiols.

© 2011 Elsevier Ltd. All rights reserved.

## 1. Introduction

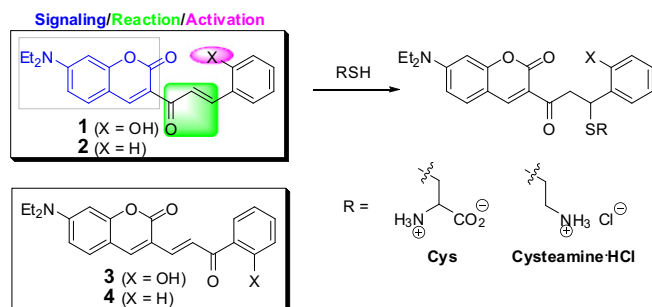
A myriad of biological processes are closely related to cellular thiols, such as cysteine (Cys), homocysteine (Hcy), and  $\gamma$ -glutamylcysteinylglycine (GSH). Cys and Hcy are involved in cellular growth,<sup>1</sup> while GSH in redox homeostasis.<sup>2</sup> Alteration in the cellular thiols is also implicated in cancer and AIDS.<sup>3</sup> Therefore, selective detection of cellular biothiols is of growing importance. Many luminescent methods have been extensively pursued due to their simplicity<sup>4</sup> and further reaction-based fluorescent probes were developed for the selective recognition of the biothiols through the Michael addition, thiazolidine formation, or disulfide exchange reaction.<sup>5</sup> In aqueous biosphere, however, the reaction is competitive with the surrounding solvents. The reaction rate is too dependent on the electronic structure of a probe to quantitatively rationalize. Hydrogen bond, especially intramolecular hydrogen bond, is a strong molecular interaction sustainable in an aqueous environment. Through the systematic investigation of intramolecular hydrogen patterns, we can understand the relationship between the structures of probes and the reaction rates and may rationally improve the rates. Until now, only a few fluorescent probes with an intramolecular hydrogen bond have been designed in viewpoint of the reaction rates in aqueous solvent.

Recently we found that the introduction of a preferable hydrogen bonding donor unit to the *ortho* position of a carbonyl group of  $\alpha,\beta$ -unsaturated enone (**3**) could accelerate the reaction rate of **3** toward 2-mercaptoethanol as fast as several dozen times compared to **4** without a hydrogen bond.<sup>6</sup> This rate acceleration is plausibly achieved through intramolecular hydrogen bonding to the oxyanion of the enolate intermediate. We wonder it is possible to activate an enone moiety by employing a hydrogen bonding donor site to a carbanion of the plausible enolate intermediate in the Michael reaction. Herein, we report that a Michael reaction is significantly affected by an intramolecular hydrogen bonding pattern. With this aim, a fluorescent probe (**1**) was prepared and compared with **3** as a Michael acceptor, where the hydroxyl group of **1** was introduced to serve as a hydrogen bonding donor to the carbanionic form of the enolate (Scheme 1). An analogue **2** without a hydroxyl group was also prepared as a reference molecule.

## 2. Results and discussion

UV–vis spectra of probe **1** are dramatically changed when **1** is treated with GSH in HEPES buffer (Fig. 1). Time-dependent UV–vis spectra of **1** (20  $\mu$ M) were monitored in the presence of 10 mM GSH. Upon the addition of GSH, a maximum peak at 472 nm ( $\epsilon=1.4\times 10^4\text{ M}^{-1}\text{ cm}^{-1}$ ) is hypsochromically shifted to 442 nm with a pseudo isosbestic point at 470 nm. The formation of **1**-GSH is apparently complete within 50 min.

\* Corresponding author. Tel.: +82 31 330 4703; fax: +82 31 330 4566; e-mail address: [haejkim@hufs.ac.kr](mailto:haejkim@hufs.ac.kr) (H.-J. Kim).



Scheme 1. The reaction of conjugated enone probes with a biothiol.

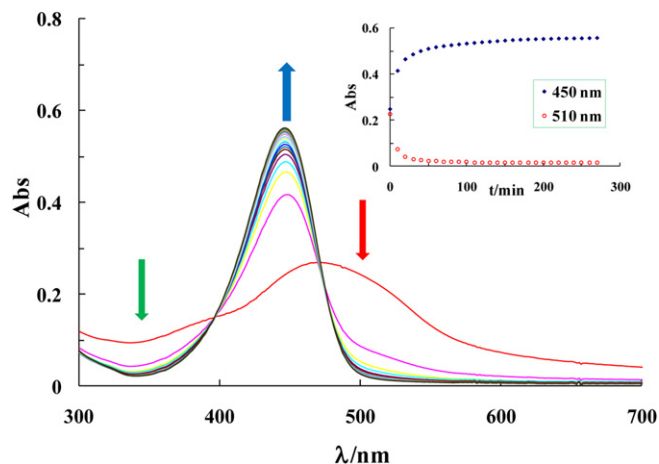


Fig. 1. Time-dependent UV–vis spectral changes of **1** (20  $\mu\text{M}$ ) with GSH (10 mM) in HEPES buffer (0.10 M, pH 7.4, 25  $^{\circ}\text{C}$ ). Inset: its kinetics.

In order to compare the reaction rates between probes (**1–4**), we carried out UV–vis kinetics at 25  $^{\circ}\text{C}$  in DMSO/HEPES buffer (Fig. 2), where **3** and **4** were also soluble. The absorbance changes at 466 nm were monitored upon the addition of GSH (10 mM) to **1** or **2** (10  $\mu\text{M}$ ) to afford the initial rate  $k$  ( $\text{M}^{-1}\text{s}^{-1}$ ) of  $8.10 \times 10^{-3}$  and  $2.85 \times 10^{-3}$  for **1** and **2**, respectively. Similar rate measurements of **3** and **4** at  $\lambda_{485\text{nm}}$  have shown the rate constant  $k$  to be  $2.35 \times 10^{-2}$  and  $9.13 \times 10^{-4} \text{ M}^{-1}\text{s}^{-1}$  for **3** and **4**, respectively (Fig. S4). The kinetic study has shown that the reaction rate of **1** was enhanced 2.8-fold compared to **2**, while the rate of **3** was enhanced as fast as 26-fold compared to **4**. The rate comparison shows that the oxyanion of **3** can be stabilized by a preferable hydrogen bond and thus the hydrogen bond induces significant rate acceleration for **3**. However, the enolate of **1** is structurally difficult to possess such a favorable hydrogen bond and thus the hydroxyl group induces a little effect on the reaction rate (Fig. 3).

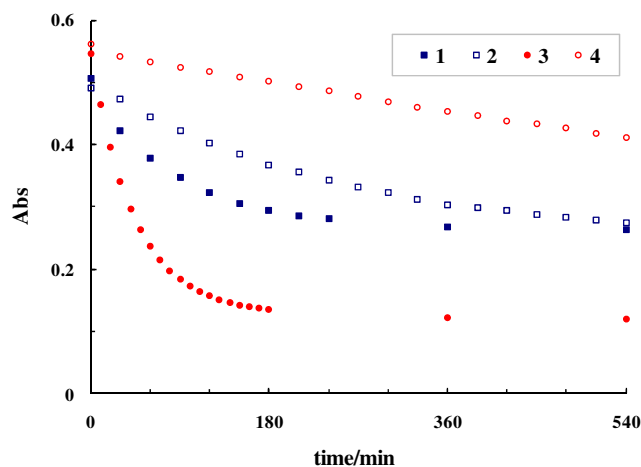


Fig. 2. Comparative UV–vis kinetics of **1–4** (10  $\mu\text{M}$ ) upon the addition of GSH (10 mM) in DMSO/HEPES buffer (4:1, v/v, 0.10 M, pH 7.4, 25  $^{\circ}\text{C}$ ).

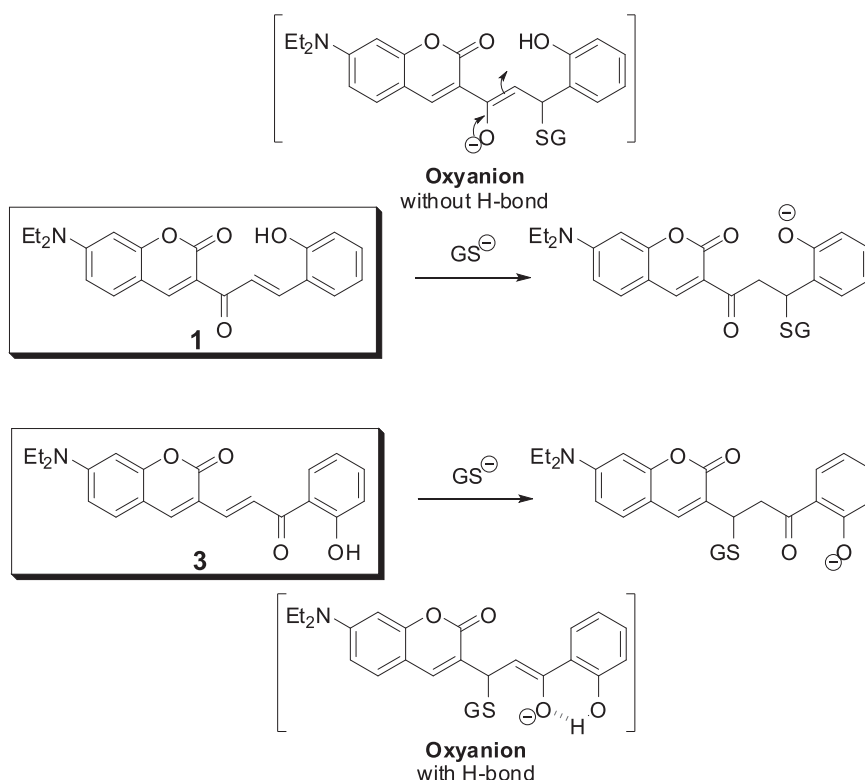


Fig. 3. Possible hydrogen bonding patterns of **1** and **3** upon the addition of GSH in HEPES buffer (pH 7.4).

Although probe **1** with an *ortho* hydroxyl group shows a slight rate enhancement relative to **2** without a hydrogen bond, it is noticeable that **1** is fairly soluble in HEPES buffer and can be applied for GSH detection in water. Upon addition of GSH, the fluorescence intensity of **1** at  $\lambda_{em}$  500 nm ( $\lambda_{ex}$  470 nm) is prominently enhanced and almost saturated around 500 equiv of GSH in HEPES buffer (0.10 M, pH 7.4). The limit of detection (LOD) of GSH was determined to be 0.14  $\mu$ M at  $3\sigma/m$ , where  $\sigma$  is the standard deviation of blank measurements and  $m$  is the slope obtained from the linear plot of **1** against GSH (Fig. 4).<sup>7</sup> According to the Job's plot, the binding stoichiometry between **1** and GSH is observed to be 1:1 (Fig. S5).

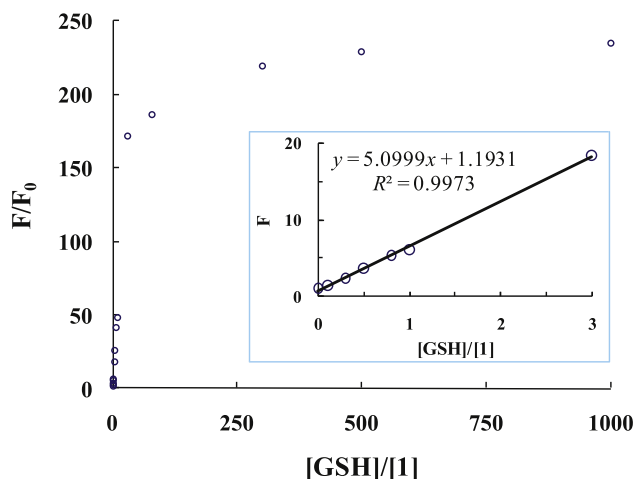


Fig. 4. Fluorescence titration curve of **1** (20  $\mu$ M) at  $\lambda_{em}/\lambda_{ex}$  500:470 nm with GSH in HEPES buffer (pH 7.4). Inset: its linear plot.

Encouraged by the UV–vis kinetics and the fluorescence experiment, we screened the selectivity of **1** toward the natural amino acids in HEPES buffer (0.10 M, pH 7.4). Only Cys shows a dramatic increase ( $F/F_0$  156) in the fluorescence intensity over other amino acids. Amino acids possessing acidic or basic side chains do not induce any significant fluorescence changes of **1** (Fig. 5A). GSH, a main biotiol component in maintaining the cellular redox homeostasis,<sup>8</sup> behaves in a similar way as Cys and enhances the fluorescence intensity of **1** ( $F_0$ ) ( $\Phi=0.0003$ ) as much as  $F/F_0=168$  ( $\Phi=0.012$  for **1**-GSH).<sup>9</sup> Competitive experiments show the consistent selectivity of **1** for GSH. The fluorescence intensity of **1** is almost restored to be as big as that of **1**-GSH upon the addition of GSH to the mixtures of **1** and other amino acid (Fig. 5B).

To investigate the reaction mechanism, <sup>1</sup>H NMR spectrum of **1** (20 mM in DMSO-*d*<sub>6</sub>) was monitored after adding 1.5 equiv cysteamine and compared with **1** itself (Fig. S3). The spectra displayed a highly upfield shift in the phenolic proton (from 10.2 to 9.6 ppm), along with the disappearance of vinylic protons upon the addition of cysteamine, which is indicative of the Michael addition reaction of cysteamine to afford **1**-cysteamine adduct. The mass spectral analysis showed corroborative evidence for the **1**-cysteamine adduct:  $m/z$  obsd 441 ( $[M+H]^+$ ), calcd 441.18 for C<sub>24</sub>H<sub>29</sub>N<sub>2</sub>O<sub>4</sub>S, Fig. S7). From the fluorescence, NMR, and mass spectral experiments, it becomes readily apparent that probe **1** selectively reacts with the thiol-containing amino acids.

The prominent luminescence changes of **1** are observable by the naked eye. Upon the addition of GSH, the **1**-GSH conjugate exhibits a color change from light yellow to green and dramatically displays a strong fluorescence, while other natural amino acids do not elicit the photophysical changes under a portable UV spectroscopy except Cys (Fig. 6). An amino acid, such as Ser does not induce any detectable fluorescence changes although it is similar to Cys in structure.

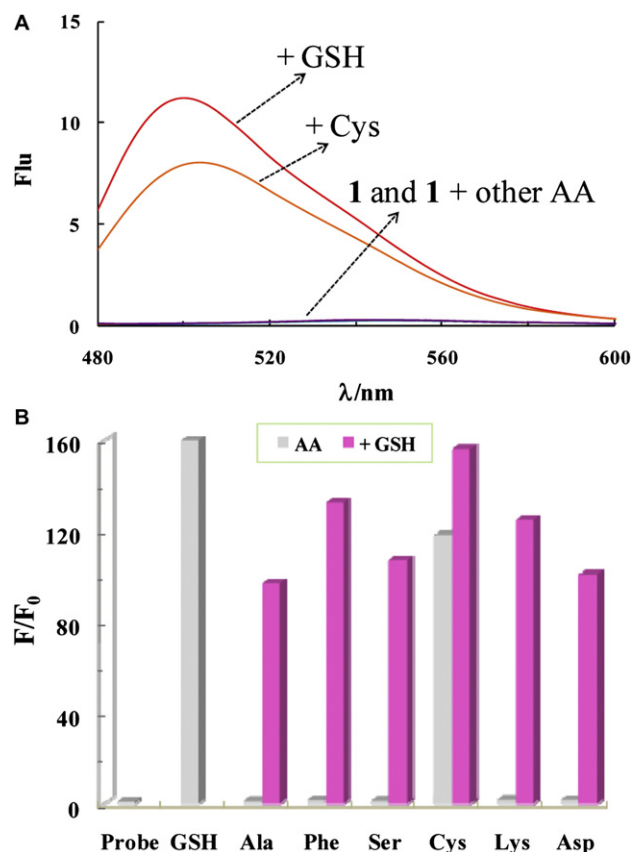


Fig. 5. (A) Fluorescence spectra of **1** (20  $\mu$ M,  $\lambda_{ex}$  470 nm) upon addition of various amino acids (AA, 500 equiv) in HEPES buffer (0.10 M, pH 7.4) and (B) their competitive fluorescence intensity changes with GSH (500 equiv) at  $\lambda_{em}$  500 nm.

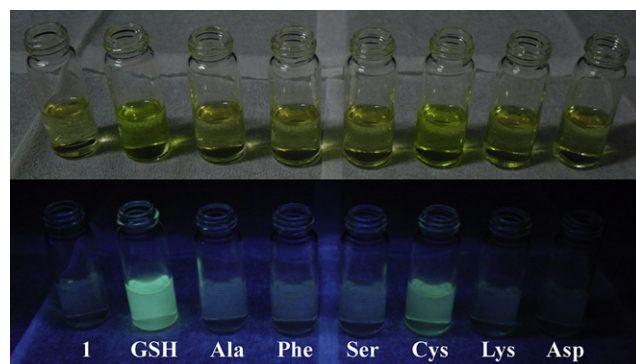


Fig. 6. Naked-eye visible and fluorescence ( $\lambda_{ex}$  365 nm) images of **1** (20  $\mu$ M) upon addition of various amino acids (AA, 500 equiv) in HEPES buffer (0.10 M, pH 7.4).

### 3. Conclusions

We prepared a series of fluorescent probes and compared their reaction rates with GSH in viewpoint of their intramolecular hydrogen bonding patterns. We found that probe **3** with an *ortho* hydroxyl group to a carbonyl group exhibits the rapidest response toward GSH owing to the stabilization of the possible oxyanion intermediate by a preferable intramolecular hydrogen bond. Probe **1** with an *ortho* hydroxyl group to the alkene of an enone, which is prone to stabilize the carbanion form of the enolate intermediate, showed a moderately enhanced reaction rate with GSH. The probe (**1**) exhibited a highly selective and sensitive fluorescence turn-on response toward biotriols even in 100% HEPES buffer.

## 4. Experimental section

### 4.1. General

All non-aqueous reactions were run in flame-dried glassware under a positive pressure of nitrogen with exclusion of moisture from reagents and glassware using standard techniques for manipulating air-sensitive compounds. Anhydrous solvents were obtained using standard drying techniques. Reactions were monitored by analytical thin-layer chromatography (TLC) performed on pre-coated, glass-backed silica gel plates. Visualization of the developed chromatogram was performed by UV absorbance, phosphomolybdic acid or iodine. Flash chromatography was performed on 230–400 mesh silica gel with the indicated solvent systems. Routine nuclear magnetic resonance spectra were recorded either on Varian Gemini 200 (200 MHz) or Varian Gemini 400 (400 MHz) spectrometers. Chemical shifts for  $^1\text{H}$  NMR spectra are recorded in parts per million from tetramethylsilane with the solvent resonance as the internal standard ( $\text{CDCl}_3$ ,  $\delta$  7.27 ppm;  $\text{DMSO}-d_6$   $\delta$  2.50 ppm). Data are reported as follows: chemical shift, multiplicity (s=singlet, d=doublet, t=triplet, q=quartet, qn=quintet, m=multiplet, and br=broad), coupling constant in hertz, and integration. Chemical shifts for  $^{13}\text{C}$  NMR spectra are recorded in parts per million from tetramethylsilane using the central peak of the solvent resonance as the internal standard ( $\text{CDCl}_3$ ,  $\delta$  77.00 ppm). All spectra were obtained with complete proton decoupling. All fluorescence and UV–vis absorption spectra were recorded in FP 6500 fluorescence spectrometer and Agilent 8453 absorption spectrometer, respectively. Mass spectra were recorded on G6401A MS-spectrometer. All experiments were carried out with commercially available reagents and solvents, and used without further purification, unless otherwise noted.

### 4.2. Kinetic analysis

The kinetic study of the probes with GSH was performed at 25 °C in DMSO/HEPES buffer (4:1, v/v, 0.10 M, pH 7.4), where all the probes are soluble. After GSH (10 mM) was added to each of the probes (10  $\mu\text{M}$ ), the absorbance changes at 466 nm (**1**, **2**) or 486 nm (**3**, **4**) were monitored. The initial rates were measured within 3 h by applying a kinetic mode in UV–vis spectrometry.

**4.2.1. (E)-7-(Diethylamino)-3-(3-(2-hydroxyphenyl)acryloyl)-2H-chromen-2-one (1).** The 3-acetyl-7-(diethylamino)-2H-chromen-2-one (0.2 g, 0.77 mmol) was dissolved in 15 mL of EtOH. Salicylic aldehyde (0.28 mL, 2.69 mmol) and piperidine (3 drops) were added at rt. The reaction mixture was refluxed for 30 h to afford a dark red solution, concentrated. Purification by column chromatography (DCM/EA/Hex=1:2:8,  $R_f$ =0.25) and recrystallization with EtOH provided product. Yield: 0.112 g (40% yield).  $^1\text{H}$  NMR (400 MHz,  $\text{DMSO}-d_6$ ):  $\delta$  10.21 (s, 1H, OH), 8.56 (s, 1H), 7.99 (d, 1H,  $J$ =16 Hz,  $-\text{COCHCH}-$ ), 7.94 (d, 1H,  $J$ =16 Hz,  $-\text{COCHCH}-$ ), 7.67 (d, 1H,  $J$ =8.8 Hz), 7.61 (d, 1H,  $J$ =6.8 Hz), 7.25 (dt, 1H,  $J$ =1.6, 8.4 Hz), 6.92 (d, 1H,  $J$ =8 Hz), 6.86 (t, 1H,  $J$ =7.6 Hz), 6.78 (dd, 1H,  $J$ =2.4, 8.8 Hz), 6.58 (d, 1H,  $J$ =2.4 Hz), 3.48 (q, 4H,  $J$ =7.2 Hz,  $-\text{NCH}_2\text{CH}_3$ ), 1.14 (t, 6H,  $J$ =7.2 Hz,  $-\text{NCH}_2\text{CH}_3$ ).  $^{13}\text{C}$  NMR (75 MHz,  $\text{DMSO}-d_6$ ):  $\delta$  186.2, 160.3, 158.6, 157.6, 153.3, 148.7, 138.0, 132.2, 128.8, 124.6, 122.0, 119.9, 116.6, 116.1, 110.5, 108.3, 96.3, 44.8, 12.8. HRMS (FAB $^+$ ,  $m$ -NBA):  $m/z$  obsd 364.1544 ( $[\text{M}+\text{H}]^+$ , calcd 364.1549 for  $\text{C}_{22}\text{H}_{22}\text{NO}_4$ ). IR (KBr,  $\text{cm}^{-1}$ ): 3255 (br), 2977 (w), 1705 (m), 1610 (m), 1580 (m), 1496 (m), 1450 (m), 1344 (m).

**4.2.2. 3-Cinnamoyl-7-(diethylamino)-2H-chromen-2-one (2).** A similar procedure was applied as **1** except that benzaldehyde was used instead of salicylaldehyde. Column chromatographic purification with EtOAc/Hex (1:1,  $R_f$ =0.50) in 30% yield.  $^1\text{H}$  NMR (200 MHz,  $\text{DMSO}-d_6$ ): 8.61 (s, 1H), 7.98 (d, 1H,  $J$ =16 Hz), 7.72 (m, 4H), 7.45 (m, 3H), 6.82 (d, 1H,  $J$ =9.0 Hz), 6.62 (s, 1H), 3.48 (q, 4H,

$J$ =6.8 Hz,  $-\text{NCH}_2\text{CH}_3$ ), 1.15 (t, 6H,  $J$ =6.8 Hz,  $-\text{NCH}_2\text{CH}_3$ ). IR (KBr,  $\text{cm}^{-1}$ ): 2975 (w), 1706 (m), 1612 (m), 1589 (m), 15,006 (m), 1444 (m), 1343 (m).

**4.2.3. 2-(3-(7-(Diethylamino)-2-oxo-2H-chromen-3-yl)-1-(2-hydroxyphenyl)-3-oxopropylthio)ethanaminium (1-cysteamine).**  $^1\text{H}$  NMR spectra of **1** (20 mM in  $\text{DMSO}-d_6$ ) were monitored upon the addition of cysteamine hydrochloride (1.5 equiv) and the reaction was almost complete within 2 days.  $^1\text{H}$  NMR (400 MHz,  $\text{DMSO}-d_6$ ):  $\delta$  9.61 (s, 1H, OHPh), 8.42 (s, 1H), 7.92 (br, 3H,  $\text{NH}_3\text{Cl}$ ), 7.63 (d, 1H,  $J$ =9.2 Hz,  $-\text{C}(\text{NEt}_2)\text{CHCHC}-$ ), 7.26 (d, 1H,  $J$ =7.6 Hz), 7.02 (t, 1H,  $J$ =7.2 Hz), 7.67 (m, 3H,  $J$ =8 Hz), 6.57 (s, 1H), 4.82 (t, 1H,  $J$ =7.2 Hz, cystamine-CH-), 3.69 (dd, 1H,  $J$ =6.8, 17.2 Hz, cystamine- $\text{CHCH}_2\text{CH}_2\text{CH}_2-$ ), 3.55 (dd, 1H,  $J$ =6.8, 17.2 Hz, cystamine- $\text{CHCH}_2\text{CH}_2\text{CH}_2-$ ), 3.50 (q, 4H,  $J$ =7.2 Hz,  $-\text{NCH}_2\text{CH}_3$ ), 3.10 (t, 2H,  $-\text{SCH}_2\text{CH}_2\text{NH}_3\text{Cl}$ ), 3.91 (t, 2H,  $-\text{SCH}_2\text{CH}_2\text{NH}_3\text{Cl}$ ), 1.14 (t, 6H,  $J$ =7.2 Hz,  $-\text{NCH}_2\text{CH}_3$ ). LRMS (FAB $^+$ ,  $m$ -NBA):  $m/z$  obsd 441 ( $[\text{M}+\text{H}]^+$ , calcd 441.18 for  $\text{C}_{24}\text{H}_{29}\text{N}_2\text{O}_4\text{S}^+$ ).

### Acknowledgements

This research was supported by the National Research Foundation funded by the Ministry of Education, Science and Technology of Korea (NRF 2008-C00206) and the Gyeonggi Regional Research Center (GRRC) program of Gyeonggi province (GRRC-HUFS-2011-B03).

### Supplementary data

Electronic Supplementary data (ESD) available: NMR and mass spectral data for compounds. Supplementary data associated with this article can be found, in the online version, at doi:10.1016/j.tet.2011.08.002.

### References and notes

- (a) Wood, Z. A.; Schroeder, E.; Harris, J. R.; Poole, L. B. *Trends Biochem. Sci.* **2003**, 28, 32; (b) Carmel, R.; Jacobsen, D. W. *Homocysteine in Health and Disease*; Cambridge University: UK, 2001.
- (a) Dalton, T. P.; Shertzer, H. G.; Puga, A. *Annu. Rev. Pharmacol. Toxicol.* **1999**, 39, 67; (b) Mathews, C. K.; van Holde, K. E.; Ahern, K. G. *Biochemistry*; Addison-Wesley Publishing Company: San Francisco, 2000.
- (a) Townsend, D. M.; Tew, K. D.; Tapiero, H. *Biomed. Pharmacother.* **2003**, 57, 145; (b) Herzenberg, L. A.; De Rosa, S. C.; Dubs, J. G.; Roederer, M.; Anderson, M. T.; Ela, S. W.; Deresinski, S. C.; Herzenberg, L. A. *Proc. Natl. Acad. Sci. U.S.A.* **1997**, 94, 1967.
- (a) Anzenbacher, P., Jr.; Try, A. C.; Miyajiri, H.; Jursikova, K.; Lynch, V. M.; Marquez, M.; Sessler, J. L. *J. Am. Chem. Soc.* **2000**, 122, 10268; (b) Miyajiri, H.; Sessler, J. L. *Angew. Chem., Int. Ed.* **2001**, 40, 154; (c) Miyajiri, H.; Sato, W.; Sessler, J. L. *Angew. Chem., Int. Ed.* **2000**, 39, 1777; (d) Xu, S.; Chen, K.; Tian, H. *J. Mater. Chem.* **2005**, 15, 2676; (e) Han, M. S.; Kim, D. H. *Tetrahedron* **2004**, 60, 11251; (f) Li, S. H.; Yu, C. W.; Xu, J. G. *Chem. Commun.* **2005**, 450; (g) Chen, H.; Zhao, Q.; Wu, Y.; Li, F.; Yi, T.; Huang, C. *Inorg. Chem.* **2007**, 46, 11075; (h) Jun, M. E.; Roy, B.; Ahn, K. H. *Chem. Commun.* **2011**, 7583.
- (a) Kantana, Y. *Angew. Chem., Int. Ed. Engl.* **1977**, 16, 137; (b) Matsumoto, T.; Urano, Y.; Shoda, T.; Kojima, H.; Nagano, T. *Org. Lett.* **2007**, 9, 3375; (c) Lin, W.; Yuan, L.; Cao, Z.; Feng, Y.; Long, L. *Chem.—Eur. J.* **2009**, 15, 5096; (d) Yi, L.; Li, H.; Sun, L.; Liu, L.; Zhang, C.; Xi, Z. *Angew. Chem., Int. Ed.* **2009**, 48, 4034; (e) Hong, V.; Kislukhin, A. A.; Finn, M. G. *J. Am. Chem. Soc.* **2009**, 131, 9986; (f) Chen, X.; Zhou, Y.; Peng, X.; Yoon, J. *Chem. Soc. Rev.* **2010**, 39, 2120; (g) Chen, X.; Ko, S.-K.; Kim, M.-J.; Shin, I.; Yoon, J. *Chem. Commun.* **2010**, 2751; (h) Zhu, B.; Zhang, X.; Li, Y.; Wang, P.; Zhang, H.; Zhuang, X. *Chem. Commun.* **2010**, 5710; (i) Shao, N.; Jin, J.; Wang, H.; Zheng, J.; Yang, R.; Chan, W.; Abliz, Z. *J. Am. Chem. Soc.* **2010**, 132, 725; (j) Jung, H. S.; Ko, K. C.; Kim, G.-H.; Lee, A.-R.; Na, Y.-C.; Kang, C.; Lee, J. Y.; Kim, J. S. *Org. Lett.* **2011**, 13, 1498; (k) Jun, M. E.; Roy, B.; Ahn, K. H. *Chem. Commun.* **2011**, 2751; (l) Long, L.; Lin, W.; Chen, B.; Gao, W.; Yuan, L. *Chem. Commun.* **2011**, 893; (m) Kwon, H.; Lee, K.; Kim, H.-J. *Chem. Commun.* **2011**, 1773.
- (a) Kim, G.-J.; Lee, K.; Kwon, H.; Kim, H.-J. *Org. Lett.* **2011**, 13, 2799; (b) Lim, S.-Y.; Kim, H.-J. *Tetrahedron Lett.* **2011**, 52, 3189; (c) Lim, S.-Y.; Lee, S.; Park, S. B.; Kim, H.-J. *Tetrahedron Lett.* **2011**, 52, 3902; (d) Park, S.; Kim, H.-J. *Chem. Commun.* **2010**, 9197.
- MacDougall, D.; Crummett, W. B. *Anal. Chem.* **1980**, 52, 2242.
- (a) Meister, A.; Anderson, M. E. *Annu. Rev. Biochem.* **1983**, 52, 711; (b) Anderson, M. E. *Chem.-Biol. Interact.* **1998**, 112, 1.
- It is remarkable that **2** ( $\Phi$ =0.0055) also showed an enhanced fluorescence intensity upon the addition of GSH ( $\Phi$ =0.0091 for **2**-GSH). However, the degree of fluorescence enhancement was observed to be very low compared to that of **1**,  $F_0/F_0 < 4.3$  (Fig. S6).